DOI: 10.1002/chem.201001208

From Metallaborane to Borylene Complexes: Syntheses and Structures of Triply Bridged Ruthenium and Tantalum Borylene Complexes

K. Geetharani,[a] Shubhankar Kumar Bose,[a] Babu Varghese,[b] and Sundargopal Ghosh*[a]

Abstract: Reaction of [1,2-(Cp*RuH)$_2$B$_3$H$_7$] (**1**; Cp* = η^5-C$_5$Me$_5$) with [Mo(CO)$_3$(CH$_3$CN)$_3$] yielded *arachno*-[(Cp*RuCO)$_2$B$_2$H$_6$] (**2**), which exhibits a butterfly structure, reminiscent of 7 sep B$_4$H$_{10}$. Compound **2** was found to be a very good precursor for the generation of bridged borylene species. Mild pyrolysis of **2** with [Fe$_2$(CO)$_9$] yielded a triply bridged heterotrinuclear borylene complex [(μ_3-BH)(Cp*RuCO)$_2$(μ-CO){Fe(CO)$_3$}] (**3**) and bis-borylene complexes [{(μ_3-BH)(Cp*Ru)(μ-CO)}$_2$Fe$_2$(CO)$_5$] (**4**) and [{(μ_3-BH)(Cp*Ru)Fe(CO)$_3$}$_2$(μ-CO)] (**5**). In a similar fashion, pyrolysis of **2** with [Mn$_2$(CO)$_{10}$] permits the isolation of μ_3-borylene complex [(μ_3-BH)(Cp*RuCO)$_2$(μ-H)(μ-CO){Mn(CO)$_3$}] (**6**). Both compounds **3** and **6** have a trigonal-pyramidal geometry with the μ_3-BH ligand occupying the apical vertex, whereas **4** and **5** can be viewed as bicapped tetrahedra, with two μ_3-borylene ligands occupying the capping position. The synthesis of tantalum borylene complex [(μ_3-BH)(Cp*TaCO)$_2$(μ-CO){Fe(CO)$_3$}] (**7**) was achieved by the reaction of [(Cp*Ta)$_2$B$_4$H$_8$(μ-BH$_4$)] at ambient temperature with [Fe$_2$(CO)$_9$]. Compounds **2**–**7** have been isolated in modest yield as yellow to red crystalline solids. All the new compounds have been characterized in solution by mass spectrometry; IR spectroscopy; and ^{1}H, ^{11}B, and ^{13}C NMR spectroscopy and the structural types were unequivocally established by crystallographic analysis of **2**–**6**.

Keywords: borylenes · manganese · metallaboranes · ruthenium · tantalum

Introduction

Metallaborane chemistry, which features compounds with direct M—B bonds, has drawn immense attention in recent years due to unusual structures, unique bonding, and varying degrees of reactivity.[1–8] On the other hand, since the advent of the first structurally authenticated bridged and terminal borylene complexes, the chemistry of this class of transition-metal complexes of boron, which displays a wealth of structural complexity and chemical reactivity, has received significant interest.[9–12] Metallaborane and borylene complexes are related to some extent because they both posses direct metal–boron bonds; however, the nature of these interactions is diverse. The cluster skeleton of a metallaborane is made up by nonclassical, electron-deficient, multicenter, two-electron bonds, whereas the borylene ligands (BR) are linked to one or two transition-metal centers by classical, electron-precise, and two-center two-electron (2c–2e) bonds.[9] Metallaboranes constitute a long recognized and well-established class of transition-metal–boron compounds that comprise several hundreds of examples;[13] however, the instability and ensuing high reactivity of borylene as a free molecule[14] signify that transition-metal–borylene complexes are challenging targets for synthetic chemists.[9,15]

Over the past decade, intense research efforts were focused on borylene complexes, and many different coordination modes for ligand of the type BR were described. These included terminal borylene species,[16] heterodinuclear complexes with bridging[17] and semibridging borylene species,[18] metalloborylenes with a bridging "naked" boron atom,[19] bis-borylene,[20] and triply bridging (μ_3-borylene)[21] species (Scheme 1). The category of μ_3-borylene complexes is restricted to very few examples that consist exclusively of homometallic frameworks of either Co[22] or Ru centers[23] and, more recently, heterometallic MnPd$_2$ systems.[21] Although

---

[a] K. Geetharani, S. K. Bose, Dr. S. Ghosh
Department of Chemistry
Indian Institute of Technology Madras
Chennai 600 036 (India)
Fax: (+91) 44-2257-4202
E-mail: sghosh@iitm.ac.in

[b] B. Varghese
Sophisticated Analytical Instruments Facility
Indian Institute of Technology Madras, Chennai 600 036 (India)

Supporting information for this article is available on the WWW under http://dx.doi.org/10.1002/chem.201001208.

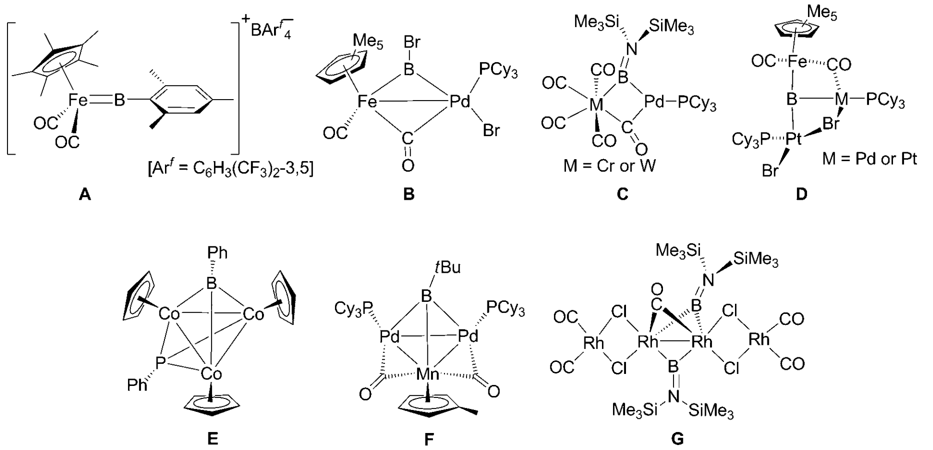

Scheme 1. Different coordination modes of borylene ligand: A) terminal, B) heterodinuclear bridged, C) semi-bridging, D) metalloborylene, E) homometallic triply bridged, F) heterometallic triply bridged, and G) bis-borylene.

diboranes(4), $X_2B–BX_2$ (X = OR, F) generally undergo oxidative additions to metal centers to give mono-, bis-, and tris-boryl complexes,[24–29] further studies by Braunschweig et al. have shown that the cleavage of the boron–boron bond in the starting diboranes(4) ($B_2X_2Cl_2$ (X = NMe_2, *t*Bu)) decisively contributes to the formation of the bridged borylene complexes.[10,30] Another approach to bridged borylene complexes was achieved by Shimoi et al. in 1998 in a similar cleavage reaction of a diborane(4) ($B_2H_4{\cdot}2PMe_3$) with $[Co_2(CO)_8]$.[31] However, the most direct access to borylene complexes is provided by salt elimination, halide abstraction, and borylene transfer.[9,32]

During the course of our studies about the reactivity of metallaboranes of early transition metals towards borane reagents ($[BH_3{\cdot}THF]$ and $[LiBH_4{\cdot}THF]$), which recently led to a general access to a series of low-boron-content metallaboranes,[33] we turned our attention to the possibility of synthesizing borylene compounds from the metallaboranes of both early- and late-transition metals. Herein we report a high-yield synthesis of *arachno*-$[(Cp^*RuCO)_2B_2H_6]$ (**2**; Cp* = η^5-C_5Me_5), a good precursor for the generation of bridged borylene compounds. In addition, we account for the synthesis of borylene species **3** and **6** and the first structurally characterized heterotrinuclear bis-borylene complexes **4** and **5**, as well as the isolation and full analytical and spectroscopic characterization of the only bridged tantalum–borylene complex, **7**. Compounds **3** and **6** represent the only ruthenium-bridged borylene species that feature the reactive borylene group B–X (X = H or Cl).

Results and Discussion

Synthesis of *arachno*-$[(Cp^*RuCO)_2B_2H_6]$ (2): The recent work on the reactivity of $[Cp^*IrB_4H_{10}]$ towards $[Mo(CO)_3(thf)_3]$ led us to investigate the reactivity of [1,2-$(Cp^*RuH)_2B_3H_7$][34] (**1**) with various monometal–carbonyl fragments. In general, the monometal–carbonyl species $[M(CO)_3(CH_3CN)_3]$ (M = Cr, Mo) are known to add metal–carbonyl fragments both in organometallic[35] and metallaborane chemistry;[36] however, compound **1** reacts in a surprisingly different fashion to yield **2**, which presumably results from the cluster degradation followed by carbonylation at the metal centers (Scheme 2). This new diruthenatetraborane has been isolated in good yield, which provides an interesting alternative to conventional methods of carbonylation[37] using monometal–carbonyl fragments. No reaction of **1** was observed with $[W(CO)_3(CH_3CN)_3]$, and all our attempts to generate **2** from $[(\eta^6\text{-arene})Cr(CO)_3]$ failed (Table 1).[38]

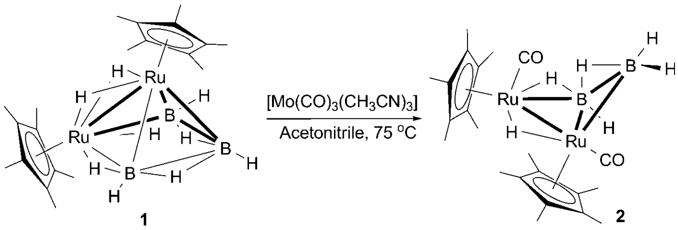

Scheme 2. Synthesis of *arachno*-$[(Cp^*RuCO)_2B_2H_6]$ (**2**) using $[Mo(CO)_3(CH_3CN)_3]$.

Table 1. Carbonylation of metallaborane [1,2-$(Cp^*RuH)_2B_3H_7$] (**1**) by monometal–carbonyl fragments.

$$[(Cp^*RuH)_2B_3H_7] \xrightarrow[\text{(M=Cr, Mo, W; } n,\ \mathbf{L} = 1,\ \text{THF; } n,\ \mathbf{L} = 3,\ CH_3CN)]{[M(CO)_{6-n}\mathbf{L}_n]} [(Cp^*RuCO)_2B_2H_6]$$

Monometal–carbonyl fragments	Solvent	*T* [°C]	*t* [h]	Yield [%][a]
$[Mo(CO)_5]{\cdot}THF$	THF	60	48	21
$[W(CO)_5]{\cdot}THF$	THF	60	18	26
$[Mo(CO)_3(CH_3CN)_3]$	CH_3CN	75	18	92
$[Cr(CO)_3(CH_3CN)_3]$	CH_3CN	75	15	74
$[W(CO)_3(CH_3CN)_3]$	CH_3CN	75	48	D[b]
$[(\eta^6\text{-arene})Cr(CO)_3]$	toluene	75	48	D[b]
CO gas	hexane	RT	02	nr[c]

[a] Yield based on Ru. [b] Decomposition. [c] No reaction.

The spectroscopic data allow **2** to be formulated as $[(Cp^*RuCO)_2B_2H_6]$ and the electron-counting rules[39] suggest a 42-electron *arachno* butterfly structure. The composition and structure of **2** have been established from elemental and mass spectral analysis, multinuclear NMR spectroscopy, and X-ray diffraction studies. The ^1H and ^{11}B NMR spectra of **2** are consistent with the solid-state X-ray structure. The FAB mass measurement of **2** gives a molecular ion that corresponds to $C_{22}H_{36}Ru_2O_2B_2$. This formulation of compound **2** rationalizes the presence of two ^{11}B resonances of equal intensity ($\delta = 21.3$ and -3.0 ppm). A peak at the lower field was assigned to the boron atom that bridges the two ruthenium metals. The $^{1}H\{^{11}B\}$ NMR spectra reveal the presence of B–H–B, Ru–H–B, and Ru–H–Ru protons; each appeared at $\delta = -3.73$, -13.15, and -15.92 ppm of intensity 1:1:1, respectively.

The molecular structure of **2**, shown in Figure 1, was arranged in a butterfly cluster in which a $[(Cp^*RuCO)_2(\mu\text{-}H)]$ fragment is bridged asymmetrically by a B_2H_5 ligand. The same coordination mode of the B_2H_5 fragment has been shown in other compounds such as $[(Cp^*IrH)_2B_2H_6]$[40] and $[(CpCo)_2(PPh_2)B_2H_5]$ ($Cp = \eta^5\text{-}C_5H_5$).[41] The existence of compound **2** permits a structural comparison with Ru, Ir, and Co analogues without the perturbations caused by additional metal fragments or ligands (Table 2). As the qualitative cluster shapes of $[(Cp^*RuCO)_2B_2H_6]$ (**2**), $[(Cp^*Ru)_2(PMe_3)B_2H_6]$,[42] $[(Cp^*IrH)_2B_2H_6]$, and $[(CpCo)_2(PPh_2)B_2H_5]$ are the same, differences are sought in the magnitude of the structural parameters. In compound **2**, the dihedral angle between the planes Ru1-B1-B2 and Ru1-B1-Ru2 is 119.3°, which is typical of *arachno*-B_4H_{10} (117.4° by electron diffraction and microwave spectroscopy),[43] Ir, and Co analogues. The bond length between Ru1 and the boron atom at the bridging position B1 (2.25(3) Å) in **2** is substantially shorter than that between Ru1 and B2 (2.32(3) Å). Similar phenomena have been observed in a number of other *arachno* molecules, such as $[(Cp^*Ru)_2(PMe_3)B_2H_6]$, $[(CpCo)_2(PPh_2)B_2H_5]$, and $[(B_6H_9)Pt_2(PMe_2Ph)_2B_2H_5]$.[44]

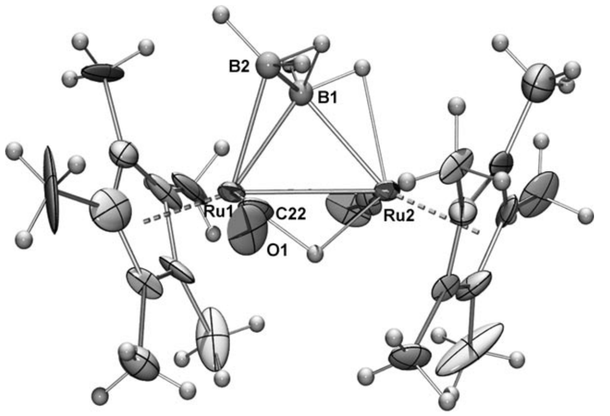

Figure 1. Molecular structure of **2**. Selected bond lengths [Å] and angles [°]: Ru1–Ru2 2.9258(10), B1–B2 1.781(17), B1–Ru1 2.25(3), B1–Ru2 2.28(3), B2–Ru1 2.32(3), Ru1–C21 1.97(3), Ru2–C22 1.79(2); B2-B1-Ru1 69.1(12), B2-B1-Ru2 113.2(19), Ru1-B1-Ru2 80.4(10), B1-Ru1-B2 45.8(6).

Utilization of *arachno*-$[(Cp^*RuCO)_2B_2H_6]$ as a precursor to borylene complexes: After developing a useful synthetic route to diruthenatetraborane **2** in good yield, a variety of reactivity patterns were investigated that have been found most profitable with metal–carbonyl fragments. As a result, mild pyrolysis of **2** with $[Fe_2(CO)_9]$ in hexane resulted in the formation of a μ_3-borylene complex **3** and μ_3-bis-borylene complexes **4** and **5** (Scheme 3). The reaction was monitored by ^{11}B NMR spectroscopy, which revealed gradual consumption of the starting material and the formation of new boron-containing compounds, as indicated by the presence of resonances in the range of $\delta = 110$–126 ppm, which are characteristic of bridged borylene ligands.[12a,b] This reaction also produced several other products that were observed during the chromatographic workup, but due to instability and insufficient amounts isolation and characterization were not possible. Descriptions of the characterization of **3**–**5** from IR spectroscopy; mass spectrometry; ^{1}H, ^{11}B, and ^{13}C NMR spectroscopy; and X-ray diffraction studies follow.

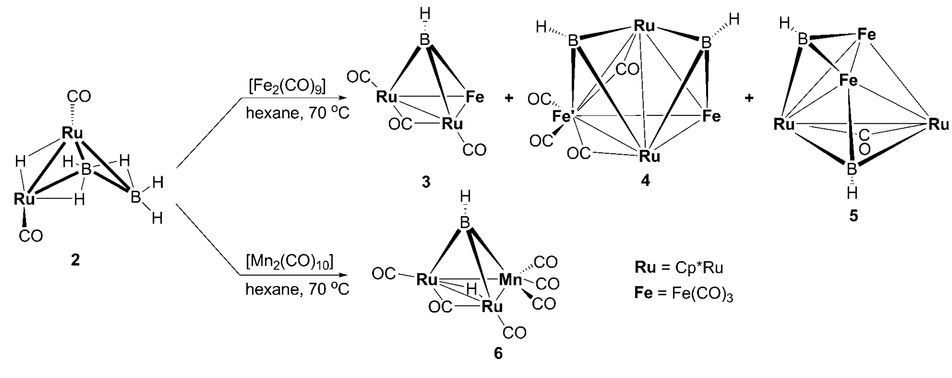

Scheme 3. Synthesis of the heterotrinuclear borylene complexes **3**–**6**.

Table 2. Comparison of the structural parameters of *arachno*-$[(Cp^*RuCO)_2B_2H_6]$ (**2**) and known dimetallatetraborane complexes.

Metallaborane	sep[a]	d(M–M) [Å]	d_{avg}(M–B) [Å]	d(B–B) [Å]	Dihedral angle [°]	δ [ppm][b] B-H-B, M-H-B	δ [ppm][c] B1, B2
$[(Cp^*RuCO)_2B_2H_6]$ (**2**)	7	2.92	2.28	1.78	119.3	−3.73, −13.15	21.3, −3.0
$[(Cp^*Ru)_2(PMe_3)B_2H_6]$	6	3.00	2.22	1.73	165.9	−2.82; −10.93, −8.45	41.5, −4.8
$[(Cp^*IrH)_2B_2H_6]$	7	2.82	2.19	1.83	115.7	−2.75, −13.99	14.2, −14.6
$[(CpCo)_2(PPh_2)B_2H_5]$	7	2.47	2.09	1.79	–[d]	−5.51, −21.15	24.2, 7.35

[a] sep = skeletal electron pairs. [b] From ^{1}H NMR spectroscopy. [c] From ^{11}B NMR spectroscopy. [d] Structural data are not available.

Characterization of $[(\mu_3\text{-}BH)(Cp^*RuCO)_2(\mu\text{-}CO)\{Fe(CO)_3\}]$ (3): The molecular-ion peak of compound **3** in the FAB mass spectrum corresponds to

$\{Cp^*_2Ru_2Fe(CO)_6BH\}$, and NMR spectroscopic data of the isolated solid are consistent with the formulation of **3**. The ^{11}B NMR spectrum displays a singlet at $\delta = 119.3$ ppm, which is shifted significantly downfield with respect to the starting material **2** ($\delta = 21.3$ ppm), thus indicating the presence of a bridging borylene ligand. The ^{1}H NMR spectrum is characterized by the presence of one singlet for the BH proton at $\delta = 9.28$ ppm and a singlet for two Cp* protons at $\delta = 1.83$ ppm. Terminal B−H and CO stretching frequencies are observed in the IR spectrum and the presence of both bridging and terminal CO ligands is confirmed by ^{13}C NMR spectroscopy.

Suitable crystals were obtained from a solution in hexane/dichloromethane (9:1) at −10 °C. The molecular structure of **3**, shown in Figure 2, was determined by single-crystal X-ray diffraction studies. In the solid-state structure of **3**, the boron atom is triply bridged by the three transition-metal atoms and lies 1.378 Å above the Ru1-Ru2-Fe1 plane. In other words, compound **3** can be viewed as a trigonal pyramid in which the three metals form a tetrahedron with the boron atom. The Ru1−Ru2 bond length of 2.7584(2) Å is in the range observed for a bond order of one but slightly longer than that in the μ_3-borylene triruthena complex $[(Cp^*Ru)_3(\mu\text{-}H)_3(\mu_3\text{-}BOEt)]$ (2.6770(5) Å).[23] The Fe−B bond length of 2.031(3) Å is longer than that observed in the metalloborylene complexes $[Cp^*(OC)Fe(\mu\text{-}CO)Pd(PCy_3)(\mu\text{-}Br)Pt(PCy_3)Br(\mu_3\text{-}B)]$ (Cy = cyclohexyl).[19] In **3**, the two carbonyl groups covalently linked to ruthenium interact with the iron center in a semibridging fashion (Ru-C_μ-O_μ 150.14(19) and 157.2(2)°, bent away from the Fe atom).

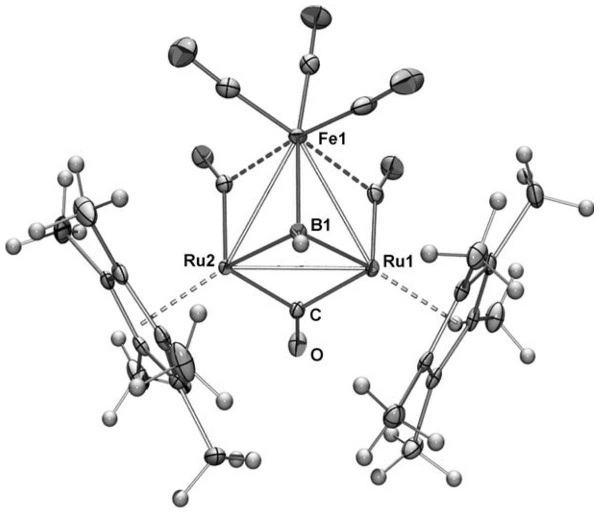

Figure 2. Molecular structure of $[(\mu_3\text{-}BH)(Cp^*RuCO)_2(\mu\text{-}CO)\{Fe(CO)_3\}]$ (**3**). Selected bond lengths [Å] and angles [°]: Ru1−Ru2 2.7584(2), Ru1−Fe1 2.6891(3), Ru2−Fe1 2.7277(4), Ru2−B1 2.140(2), Ru1−B1 2.1052, Fe1−B1 2.031(3); Ru1-Fe1-Ru2 61.220(8), Ru1-B1-Ru2 81.05(9).

Characterization of $[\{(\mu_3\text{-}BH)(Cp^*Ru)(\mu\text{-}CO)\}_2Fe_2(CO)_5]$ (4): Compound **4** was isolated as a brown, air-stable solid. The mass spectrometric data suggest a molecular formula of $\{Cp^*_2Ru_2Fe_2(CO)_7B_2H_2\}$, and the ^{11}B and ^{1}H NMR spectroscopic data suggest a structure, if static, of higher symmetry. Compound **4** displays a single resonance at $\delta = 125.4$ ppm in the ^{11}B NMR spectrum, which is close to the range observed for triply bridged borylene complexes.[21,23] Consistent with this observation, the ^{13}C NMR spectrum also shows one Cp* signal. The presence of a bridging and terminal CO groups are established by the characteristic signals at $\delta = 212.3$ and 201.9 ppm in the ^{13}C NMR spectrum and by CO stretching frequencies in the IR spectrum.

The atom connectivity within the compounds was persuasively determined by performing a single-crystal X-ray diffraction study of **4** (Figure 3). It consists of a Ru_2Fe_2 isosceles tetrahedron (bond lengths: Ru1−Ru2 2.7954(4), Ru1−Fe3 2.5912(6), Ru1−Fe4 2.6623(6), Fe3−Fe4 2.6216(7) Å), in which two of the faces (Ru1-Ru2-Fe3 and Ru1-Ru2-Fe4) are symmetrically bridged by the borylene ligand (BH) in a μ_3 fashion. The average B−Ru distance of 2.089 Å lies in the range of those reported for the transition-metal borylene complexes.[45] The two borylene ligands B1H and B2H lie 1.416 and 1.389 Å above the metal triangular planes, respectively. The average dihedral angle between the plane of B1-Fe3-Fe4-B2 atoms relative to the Cp* ligands is 145.1°, whereas the tilt of the plane of two Cp* ligands is 110.3°.

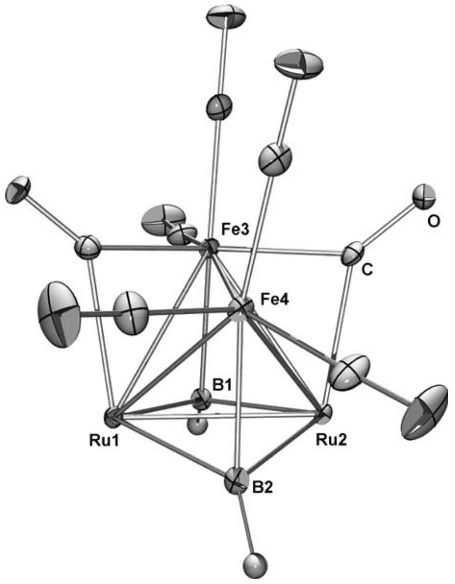

Figure 3. Molecular structure of $[\{(\mu_3\text{-}BH)(Cp^*Ru)(\mu\text{-}CO)\}_2Fe_2(CO)_5]$ (**4**; Cp* ligands omitted for clarity). Selected bond lengths [Å] and angles [°]: Ru1−Ru2 2.7954(4), Ru1−Fe3 2.5912(6), Ru1−Fe4 2.6623(6), Fe3−Fe4 2.6216(7), Ru2−Fe4 2.7018(6), Ru1−B1 2.078(5), Fe3−B1 2.140(4), Ru1−B2 2.092(5), Fe4−B2 2.078(4); Ru1-Fe3-Ru2 65.113(15), Ru1-B1-Ru2 84.78(16), Ru1-Fe4-Ru2 62.812(14), Ru1-B2-Fe4 79.36(17).

Characterization of $[\{(\mu_3\text{-}BH)(Cp^*Ru)Fe(CO)_3\}_2(\mu\text{-}CO)]$ (5): Compound **5** has been isolated following TLC and characterized in comparison to their spectroscopic data with the similarly bridged borylene species **4**. The mass spectrometric data suggested a molecular formula of $C_{27}H_{32}B_2Fe_2O_7Ru_2$. The IR spectrum of **5** is distinguished by the presence of a strong absorption due to terminal and bridging CO ligands that appear at 1900–2000 and 1726 cm^{-1}, respectively. The ^{11}B NMR spectrum indicates the presence of two boron environments in a ratio of 1:1 at $\delta = 121.3$ and 110.6 ppm, thus indicating the presence of two unsymmetrical bridging borylene ligands. Furthermore, the ^{1}H NMR spectrum reveals the presence of two Cp* resonances and two terminal B−H protons in the ratio of 1:1. The ^{13}C NMR spectrum indicates the presence of carbonyl ligands due to signals at $\delta = 215.1$ and 213.9 ppm.

Single crystals suitable for X-ray diffraction analysis of **5** were obtained from a hexane solution at −4 °C. The framework geometry of **5** is shown in Figure S1 in the Supporting Information. Complex **5** crystallizes in the space group $Pna2_1$, and the structure exhibits a metal–metal bonded, tetrahedral geometry of Ru_2Fe_2, in which each Ru atom is bound to a Cp* ligand and each Fe atom is bound to carbonyl ligands. The two different triangular faces Ru1-Fe1-Ru2 and Ru1-Fe1-Fe2 are capped by a borylene ligand (BH) in a μ_3 fashion. The interatomic distance Ru1−Ru2 of 2.703 Å clearly indicates the existence of a single bond between the ruthenium atoms; however, it is slightly shorter than that observed in **3** and **4**. The dihedral angle between the two three-membered rings, Ru1-B1-Fe1 and Ru1-B2-Fe1, is 176.7°. The Fe1−B1 and Fe2−B2 bond lengths are 1.98(2) and 1.842(12) Å, respectively. These are considerably shorter than that found in the boryl complex $[CpFe(CO)_2BPh_2]$ (2.034(3) Å)[46] and bridged borylene complex $[(\eta\text{-BN(SiMe}_3)_2)(\mu\text{-CO})\{Cp^{+}Fe(CO)\}_2]$ (2.007(3) and 2.002(3) Å) ($Cp^{+} = (\eta^5\text{-}C_5H_4Me)$).[47]

Bis(borylene) complexes are limited to only the tetranuclear rhodium complex $[Rh_4\{\mu\text{-BN(SiMe}_3)_2\}_2(\mu\text{-Cl})_4(\mu\text{-CO})(CO)_4]$, which consists of four rhodium atoms in a chain, and the internal metal centers are bridged by two bridging aminoborylene moieties.[20] Both compounds **4** and **5** can be viewed as heterometallic bis-borylene species. On the basis of the capping principle, the skeletal electron count is determined by the central polyhedron (i.e., Ru_2Fe_2 tetrahedron). A formal electron count[39] for both **4** and **5** is in agreement with the metallaborane $[(Cp^{*}Re)B_4H_8]$,[48] that is, six skeletal electron pairs (sep) appropriate for tetrahedral geometry.

Reactivity of 2 with $[Cp^{*}Re(CO)_3]$, $[Co_2(CO)_8]$, and $[Mn_2(CO)_{10}]$: The comparison of isoelectronic species is an old but powerful method for identifying similarities between the electronic structures of compounds of different atomic compositions.[49] The differences are key and highlight the real possibilities of the exploitation of element variation in the articulate control of chemical properties.[50] Thus, in an attempt to further exploit the synthesis of bridged borylene complexes, other sources of metal–carbonyl fragments were investigated. Accordingly, a solution of **2** in hexane was pyrolyzed independently in the presence of $[Cp^{*}Re(CO)_3]$, $[Co_2(CO)_8]$, and $[Mn_2(CO)_{10}]$ at 70 °C. Although the objective of the generation of bridged borylene species was not achieved in the cases of Re and Co, $[Mn_2(CO)_{10}]$ generated the new heterometallic μ_3-borylene complex $[(\mu_3\text{-BH})(Cp^{*}RuCO)_2(\mu\text{-H})(\mu\text{-CO})\{Mn(CO)_3\}]$ (**6**) (Scheme 3). After recrystallization in hexane, **6** was isolated as highly air- and moisture-sensitive red crystals in 28 % yield.

The FAB mass analysis of **6** gives a molecular-ion peak that corresponds to $\{Cp^{*}_2Ru_2Mn(CO)_6BH_2\}$. Both ^{11}B and ^{1}H NMR spectra of **6** indicate a highly symmetrical molecule. In particular, note the ^{11}B chemical shift ($\delta = 89$ ppm) that suggests a boron atom in a highly metallic environment and the highfield ^{1}H resonance ($\delta = -6.37$ ppm) that suggests the presence of an Ru-H-Ru bridging hydride. In addition to the resonances due to the BH proton, the ^{1}H NMR spectrum also reveals a peak at $\delta = 2.08$ ppm for the Cp* protons, thus indicating identical Ru environments. The IR spectrum of **6** is consistent with a structure that features five terminally bound and one bridged carbonyl ligands (confirmed by the ^{13}C NMR spectrum).

The solid-state X-ray structure of **6** is shown in Figure 4, in which it can be seen that the compound has a *closo*-tetrahedral cluster geometry. The structure of **6** exhibits an equilateral triangle array of one Mn and two Ru atoms capped on one side by a μ_3-BH fragment. The core geometry of **6** is analogous to that observed for **3**, and the triply bridged boron atom lies 1.436 Å above the Ru1-Ru2-Mn1 plane. The Mn−B bond (2.115(5) Å) is shorter than in haloborylene complex $[\{(CO)_5Mn\}_2(\mu\text{-BBr})]$ (2.156 Å) and slightly longer than other related boryl complexes.[51] The Ru−Ru and Ru−B distances are within the range expected for either hydrogen-bridged or unbridged edges. The Ru-H-Ru hydrogen atom was not located, however; this was confirmed by the low-temperature $^{1}H\{^{11}B\}$ NMR spectrum. Compound **6**

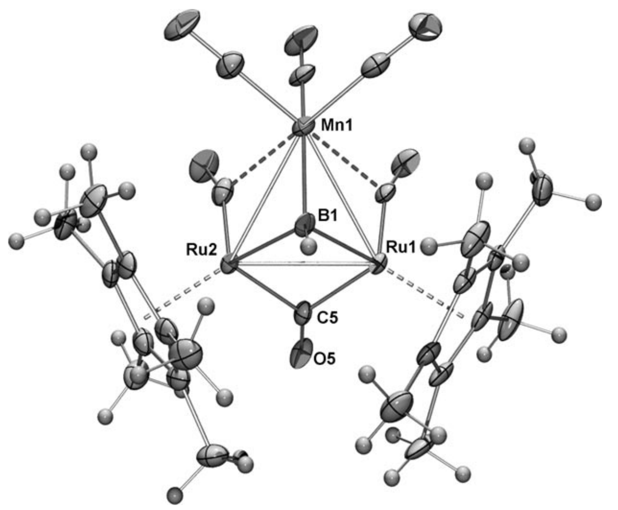

Figure 4. Molecular structure of $[(\mu_3\text{-BH})(Cp^{*}RuCO)_2(\mu\text{-H})(\mu\text{-CO})\{Mn(CO)_3\}]$ (**6**). Selected bond lengths [Å] and angles [°]: Ru1−Ru2 2.7789(5), Ru1−Mn1 2.7970(8), Ru2−Mn1 2.7777(8), Ru1−B1 2.191(6), Mn1−B1 2.115(5); Ru1-Mn1-Ru2 59.798(18), Ru1-B1-Ru2 79.4(2).

contains two semibridging carbonyl ligands that link the Cp*Ru and $Mn(CO)_3$ fragments.

Bridged borylene complexes of tantalum: After discovering that the reaction of *arachno*-**2** with $[Fe_2(CO)_9]$ and $[Mn_2(CO)_{10}]$ led to the isolation of heterometallic μ_3-borylene and bis-borylene complexes **3**–**6**, an investigation of the tantalum system became attractive. As the structural core of bis-borylene complexes **4** and **5** is somewhat similar to $[(Cp^*Ta)_2B_4H_8(\mu\text{-}BH_4)]$,[33b] an addition reaction of the metal–carbonyl fragment to this tantalum system was examined. The reaction of $[(Cp^*Ta)_2B_4H_8(\mu\text{-}BH_4)]$ with an excess amount of $[Fe_2(CO)_9]$ under mild reaction conditions yielded **7** in parallel with known $[(Cp^*Ta)_2B_5H_{11}]$.[33a] The geometry of this new compound is established in comparison to its spectroscopic data with **3**, **6**, and other related species.[23]

The composition of **7** is defined by the mass, an isotopic distribution pattern that is characteristic of one B, one Fe, and two Ta atoms. It is also evident by six envelopes that correspond to the successive loss of CO from the parent-ion mass of 867. The ^{11}B and ^{1}H NMR spectra of **7** indicate a highly symmetrical molecule, and they are very similar to that of **3** and **6**. The ^{11}B NMR spectrum features a broad signal at $\delta = 119.5$ ppm, which is consistent with a bridging borylene ligand, and the chemical shift is similar to that observed for **3** ($\delta = 119.3$ ppm). The IR spectrum of **7** exhibited a medium absorption at 2498 cm^{-1}, which is characteristic of a terminal B–H stretch. In addition, compound **7** exhibits three absorption bands, two that correspond to terminal carbonyl (2017 (s), 1954 cm^{-1} (vs)) and one corresponding to a bridging carbonyl (1745 cm^{-1} (s)). The presence of one terminal hydrogen (BH) is also confirmed by the ^{1}H NMR spectrum, which shows a broad resonance at $\delta = 9.4$ ppm and one sharp signal for the two chemically equivalent Cp* ligands (confirmed by ^{13}C NMR spectroscopy). From the mass-spectral analysis combined with the ^{11}B, ^{1}H, and ^{13}C NMR spectrum, **7** is described as a heterotrinuclear, triply bridged tantalum borylene complex $[(\mu_3\text{-}BH)(Cp^*TaCO)_2(\mu\text{-}CO)\{Fe(CO)_3\}]$. Despite many unsuccessful attempts to grow crystals of **7** of X-ray quality, the molecular formula as well as the spectroscopic properties of **7** is best fit with the proposed structure as shown in Scheme 4.

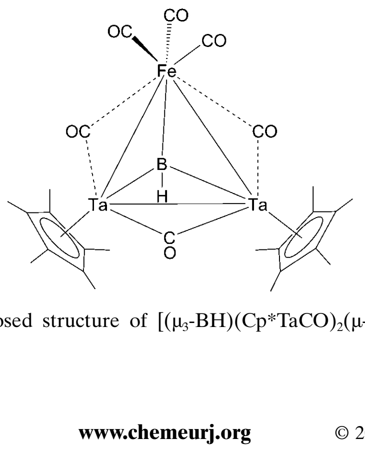

Scheme 4. Proposed structure of $[(\mu_3\text{-}BH)(Cp^*TaCO)_2(\mu\text{-}CO)\{Fe(CO)_3\}]$ (**7**).

Substitution of H with Cl in 3 and 6: In contrast to the similarities with respect to their molecular structures, **3** and **6** show markedly different stability, as already indicated by the extreme sensitivity of **6**, which stands in stark contrast to the stability of **3** even towards air and moisture. Both the borylene species proved unreactive towards HCl and MeOH; however, they underwent a clean, albeit slow, reaction with $[BHCl_2{\cdot}SMe_2]$ in toluene at 80 °C to yield monochloro derivative $[(\mu_3\text{-}BCl)(Cp^*RuCO)_2(\mu\text{-}H)_n(\mu\text{-}CO)\{M(CO)_3\}]$ (in which M = Fe, $n = 0$; M = Mn, $n = 1$). The products of the reactions of **3** and **6** with $[BHCl_2{\cdot}SMe_2]$ were observed by ^{11}B and ^{1}H NMR spectroscopy, and the spectra showed evidence of the substitution of a terminal hydrogen atom by a chlorine atom. In an attempt to derivatize the bis-borylene complexes, **4** and **5** were treated with MeOH at 80 °C. However, no derivatization reaction was observed. Instead they cleanly led to the formation of **3**.

Geometrical and spectroscopic comparison of borylene species 3–7: The main-group transition-metal element clusters mimic structural aspects of metal clusters, metal hydroborate complexes, and metal–hydrocarbon π complexes.[52] Both isolobal analogies and cluster electron-counting protocols are now strongly established as conceptual, as well as practical tools of the modern chemist. Clusters **3** and **6** with an M_3B core geometry of trigonal-pyrimidal permit a comparison with the isoelectronic clusters $[Co_3(CO)_9(\mu_3\text{-}CCH_3)]$,[53] $[Fe_3(\mu\text{-}H)_3(CO)_9(\mu_3\text{-}CCH_3)]$,[54] and $[HFe_3(CO)_9BH_3R]$[55] (R = H, CH_3). With the exception of the tantalum borylene species **7**, all the clusters (shown in Scheme 5) have a polyhedral electron count (pec) of 50 (pec of **7** = 44). Hence, the synthesis of main-group element analogues provides an experimental platform for the development and understanding of the role of element variation in both structure and reactivity.[2]

The foundation of the borylene complexes **3**–**7** in solution was derived from spectroscopic data (Table 3). In case of all borylene complexes, lowfield-shifted ^{11}B NMR spectroscopic

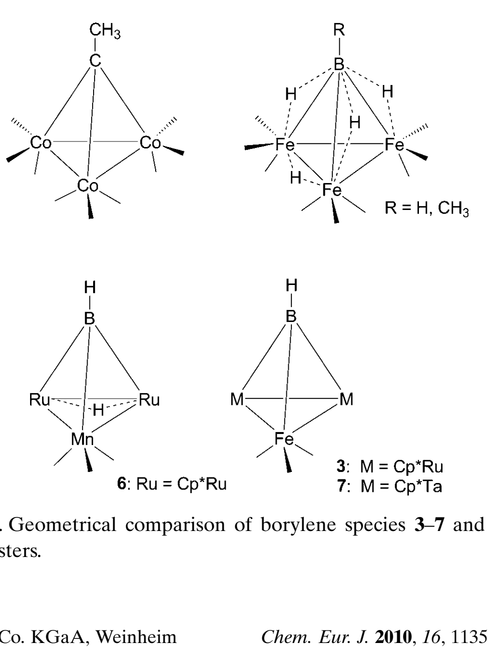

Scheme 5. Geometrical comparison of borylene species **3**–**7** and isoelectronic clusters.

Table 3. Selected structural parameters and chemical shifts (^{1}H and ^{11}B NMR spectra) of **3–7** and other related clusters.

Borylene complex	^{11}B NMR δ [ppm]	$\tilde{\nu}_{CO}$ [cm^{-1}]	d_{avg}(M−B) [Å]	d(B−R) [Å]
$[(\mu^3\text{-BH})(\text{Cp*RuCO})_2(\mu\text{-CO})\{\text{Fe(CO)}_3\}]$ (**3**)	119.3	2020, 1971, 1743	2.092	1.10[a]
$[\{(\mu^3\text{-BH})(\text{Cp*Ru})(\mu\text{-CO})\}_2\text{Fe}_2(\text{CO})_5]$ (**4**)	125.4	2021, 1979, 1937, 1730	2.089, 2.109	1.14[a]
$[\{(\mu^3\text{-BH})(\text{Cp*Ru})\text{Fe(CO)}_3\}_2(\mu\text{-CO})]$ (**5**)	121.3, 110.6	2005, 1968, 1933, 1726	2.093, 2.144	1.29[a]
$[(\mu^3\text{-BH})(\text{Cp*RuCO})_2(\mu\text{-H})(\mu\text{-CO})\{\text{Mn(CO)}_3\}]$ (**6**)	89	2013, 1943, 1736	2.155	0.87[a]
$[(\mu^3\text{-BH})(\text{Cp*TaCO})_2(\mu\text{-CO})\{\text{Fe(CO)}_3\}]$ (**7**)	119.5	2017, 1954, 1745	–	–[b]
$[(\text{CpCo})_3\text{PPhBPh}]\cdot 0.5\,\text{C}_6\text{H}_6$	143.7	–	2.038	–[c]
$[(\text{Cp*Ru})_3(\mu\text{-H})_3(\mu^3\text{-BOEt})]$	87.7	–	2.154	1.374
$[(\mu^3\text{-B}t\text{Bu})\{[\text{Cp+Mn(CO)}_2][\text{Pd(PCy}_3)]_2\}]$	150	1811, 1770	2.086	1.601
$[(\text{Cp*Co})_3(\mu^3\text{-HBH})_2]$[56]	104	–	1.999	–[c]

[a] Borylene ligands **3–6** in which R = H. [b] All attempts to grow better X-ray quality crystals of **7** failed without significant improvement of crystal data. [c] No details of the structure in the crystal are available.

signals that ranged from about $\delta = 87$–150 ppm were observed. This significant deshielding resonance is characteristic for all triply bridged borylene complexes.

Conclusion

A highly efficient synthetic route to *arachno*-$[(\text{Cp*RuCO})_2\text{B}_2\text{H}_6]$ (**2**) has been developed by the reaction of $[(\text{Cp*RuH})_2\text{B}_3\text{H}_7]$ and monometal–carbonyl fragments $[\text{M(CO)}_3(\text{CH}_3\text{CN})_3]$ (M = Cr, Mo). The chemistry of transition-metal–borylene complexes has come a long way since the discovery of the first structurally characterized systems more than a decade ago. The progress of a variety of synthetic approaches has broadened the extent of available systems, both in terms of the borylene substituent and the range of attuned metal–ligand frameworks. Herein we have demonstrated for the first time that a metallaborane species, *arachno*-**2**, can be utilized appropriately as a precursor to heterotrinuclear compounds, which comprise triply bridged borylene and bis-borylene ligands, a relatively rare structural motif. As demonstrated herein in the isolation of the first tantalum borylene and ruthenium bis-borylene species, the ability to tune the metal fragment over a considerable range of transition metals permits the manipulation of heteronuclear bridged borylene compounds. Furthermore, the *exo*-cluster substitution at B−H in the borylene species was carried out cleanly by using $[\text{BHCl}_2\cdot\text{SMe}_2]$, which could be useful in preparing functionalized clusters for assembly into larger arrays. The study of the reactivity of these and analogous species is currently underway in our laboratories.

Experimental Section

General procedures and instrumentation: All manipulations were conducted either under an atmosphere of dry argon inside a glove box or by employing standard Schlenk techniques. Solvents were distilled prior to use under argon. $[(\text{Cp*RuCl}_2)_2]$, $[\text{Cp*TaCl}_4]$, $[\text{Cp*Re(CO)}_3]$, $[\text{Mo(CO)}_6]$, $[\text{Cr(CO)}_6]$, $[\text{W(CO)}_6]$, $[\text{Fe}_2(\text{CO})_9]$, $[\text{Mn}_2(\text{CO})_{10}]$, $[\text{Co}_2(\text{CO})_8]$, $[\text{BH}_3\cdot\text{THF}]$, and LiBH_4 in THF (Aldrich) were used as received. The compounds *nido*-$[1,2\text{-(Cp*RuH)}_2\text{B}_3\text{H}_7]$,[34] $[\text{M(CO)}_3(\text{CH}_3\text{CN})_3]$ (M = Mo, Cr and W),[57] $[\text{M(CO)}_5]\cdot\text{THF}$ (M = Mo and W),[58] and $[(\eta^6\text{-arene})\text{Cr(CO)}_3]$[59] were prepared as described in the literature. The external reference for the ^{11}B NMR spectroscopy, $[\text{Bu}_4\text{N}(\text{B}_3\text{H}_8)]$, was synthesized with the literature method.[60] Thin-layer chromatography was carried out on 250 mm diameter aluminum-supported silica-gel TLC plates (MERCK TLC Plates). NMR spectra were recorded using 400 and 500 MHz Bruker FT-NMR spectrometers. Residual solvent protons were used as reference ([D$_6$]benzene, $\delta = 7.16$ ppm), whereas a sealed tube containing $[\text{Bu}_4\text{N}(\text{B}_3\text{H}_8)]$ in [D$_6$]benzene ($\delta_B = -30.07$ ppm) was used as an external reference for the ^{11}B NMR spectroscopy. Infrared spectra were recorded using a Nicolet 6700 FT spectrometer. Microanalyses for C, H, and N were performed using Perkin–Elmer Instruments series II model 2400. Mass spectra were obtained using a JEOL JMS-AX505HA mass spectrometer with perfluoro kerosene as standard and a Jeol SX 102 Da-600 mass spectrometer using argon/xenon (6 kv, 10 mÅ) as the FAB gas.

General procedure for synthesis of 2: In a typical preparation, a solution of $[1,2\text{-(Cp*RuH)}_2\text{B}_3\text{H}_7]$ (0.13 g, 0.25 mmol) in acetonitrile (20 mL) was thermolyzed with an excess amount of $[\text{Mo(CO)}_3(\text{CH}_3\text{CN})_3]$ at 75 °C for 18 h. The solvent was evaporated in vacuo; residue was extracted into hexane and passed through Celite mixed with small amount of silica gel. After removal of solvent from filtrate, the residue was subjected to chromatographic workup using silica-gel TLC plates. Elution with hexane/CH_2Cl_2 (8:2 v/v) yielded yellow $[(\text{Cp*RuCO})_2\text{B}_2\text{H}_6]$ (**2**; 0.13 g, 92 %). ^{11}B NMR (128 MHz, [D$_6$]benzene, 22 °C): $\delta = 21.3$ (brs, 1 B), −3.0 ppm (brs, 1 B); ^{1}H NMR (400 MHz, [D$_6$]benzene, 22 °C): $\delta = 3.39$ (partially collapsed quartet (pcq), 1 BH$_t$), 2.80 (pcq, 1 BH$_t$), 2.43 (pcq, 1 BH$_t$), 1.81 (s, 15 H; C$_5$Me$_5$), 1.75 (s, 15 H; C$_5$Me$_5$), −3.73 (s, in ^{1}H–^{11}B decouple, 1 B-H-B), −13.15 (s, in ^{1}H–^{11}B decouple, 1 Ru-H-B), −15.92 ppm (s, in ^{1}H-^{11}B decouple, 1 Ru-H-Ru); ^{13}C NMR (100 MHz, [D$_6$]benzene, 22 °C): $\delta =$ 208.2 and 203.1 (CO), 97.1 and 95.4 (C_5(CH$_3$)$_5$), 9.9 and 8.9 ppm (C$_5$(CH$_3$)$_5$); IR (hexane): $\tilde{\nu} = 2443$ (w), 2407 (w, B−H$_t$), 1921 cm^{-1} (s, Ru−CO); MS (FAB): m/z P^+_{max}: 555 (isotopic pattern for 2 Ru, 2 CO, and 2 B atoms); elemental analysis calcd (%) for $\text{C}_{22}\text{H}_{36}\text{B}_2\text{Ru}_2\text{O}_2$: C 47.50, H 6.52; found: C 48.01, H 6.91.

Synthesis of 3, 4, and 5: A solution of **2** (0.15 g, 0.27 mmol) in hexane (15 mL) was stirred at 70 °C in presence of $[\text{Fe}_2(\text{CO})_9]$ (0.29 g, 0.81 mmol, 3 equiv) for 2 h. The solvent was removed in vacuo; the residue was extracted into hexane and passed through Celite. The filtrate was concentrated and kept at −40 °C to remove $[\text{Fe}_3(\text{CO})_{12}]$. The mother liquor was concentrated and the residue was chromatographed on silica-gel TLC plates. Elution with hexane/CH_2Cl_2 (8:2 v/v) mixture yielded reddish brown **3** (0.03 g, 16 %), **4** (0.05 g, 23 %), and **5** (0.08 g, 37 %).

Compound 3: ^{11}B NMR (128 MHz, [D$_6$]benzene, 22 °C): $\delta = 119.3$ ppm (br, 1 B); ^{1}H NMR (400 MHz, [D$_6$]benzene, 22 °C): $\delta = 9.28$ (br, 1 BH$_t$), 1.83 ppm (s, 30 H; Cp*); ^{13}C NMR (100 MHz, [D$_6$]benzene, 22 °C): $\delta =$ 214.6, 205.1 (CO), 101.2 (C_5(CH$_3$)$_5$), 9.6 ppm (C$_5$(CH$_3$)$_5$); IR (hexane): $\tilde{\nu} = 2471$ (w, B−H$_t$), 2020, 1971, 1743 cm^{-1} (CO); MS (FAB): m/z P^+_{max}: 709; elemental analysis calcd (%) for $\text{C}_{26}\text{H}_{31}\text{B}_1\text{Fe}_1\text{Ru}_2\text{O}_6$: C 44.08, H 4.41; found: C 43.61, H 4.62.

Compound 4: ^{11}B NMR (128 MHz, [D$_6$]benzene, 22 °C): $\delta = 125.4$ ppm (br, 2 B); ^{1}H NMR (400 MHz, [D$_6$]benzene, 22 °C): $\delta = 8.59$ (br, 2 BH$_t$), 1.83 ppm (s, 30 H; Cp*); ^{13}C NMR (100 MHz, [D$_6$]benzene, 22 °C): $\delta =$

Table 4. Crystallographic data and structure refinement information for compounds **2–4** and **6**.

	2	**3**	**4**	**6**
empirical formula	$C_{22}H_{36}B_2O_2Ru_2$	$C_{26}H_{31}BFeO_6Ru_2$	$C_{27}H_{32}B_2Fe_2O_7Ru_2$	$C_{26}H_{31}BMnO_6Ru_2$
formula weight	556.27	708.31	803.99	707.40
crystal system	monoclinic	monoclinic	monoclinic	monoclinic
space group	*Cc*	*P*21/*n*	*Pn*	$P2_1/c$
a [Å]	16.2297(10)	9.5330(2)	9.2049(2)	11.5634(4)
b [Å]	8.2031(6)	17.4379(4)	11.3156(4)	13.2128(4)
c [Å]	19.0572(13)	16.1187(4)	13.8309(4)	17.4891(8)
α [°]	90.00	90.00	90	90.00
β [°]	110.260(3)	100.2300(10)	92.3560(10)	93.757(4)
γ [°]	90.00	90.00	90	90.00
V [Å^3]	2380.2(3)	2636.90(10)	1439.39(7)	2666.33(17)
Z	4	4	2	4
ρ_{calcd} [g cm^{-3}]	1.552	1.784	1.855	1.762
F(000)	1128	1416	800	1412
μ [mm^{-1}]	1.283	1.713	2.061	1.623
crystal size [mm]	0.20 × 0.10 × 0.10	0.22 × 0.21 × 0.19	0.38 × 0.25 × 0.22	0.28 × 0.21 × 0.17
θ range [°]	2.28-25.00	1.74-25.00	1.80-28.31	3.02-25.00
no. of total reflns collected	11519	15409	10220	18753
no. of unique reflns ($I > 2\sigma(I)$)	3850	4288	5660	4686
data/restraints/params	3850/63/263	4288/0/339	5660/2/379	4686/0/339
goodness-of-fit on F^2	1.134	1.101	1.085	1.030
final *R* indices ($I > 2\sigma(I)$)	$R_1 = 0.0509$ $wR_2 = 0.1234$	$R_1 = 0.0168$ $wR_2 = 0.0395$	$R_1 = 0.0214$ $wR_2 = 0.0437$	$R_1 = 0.0433$ $wR_2 = 0.1121$
R indices (all data)	$R_1 = 0.0678$ $wR_2 = 0.1335$	$R_1 = 0.0197$ $wR_2 = 0.0415$	$R_1 = 0.0230$ $wR_2 = 0.0514$	$R_1 = 0.0508$ $wR_2 = 0.1147$
largest difference in peak and hole [e Å^{-3}]	1.584 and −1.317	0.359 and −0.304	0.459 and −0.462	1.162 and −1.391

212.3, 201.9 (CO), 102.2 ($C_5(CH_3)_5$), 10.1 ppm ($C_5(CH_3)_5$); IR (hexane): $\tilde{\nu} = 2499$ (w, B−H$_t$), 2021, 1979, 1937, 1730 cm^{-1} (CO); MS (FAB): *m*/*z* P^+_{max}: 803; elemental analysis calcd (%) for $C_{27}H_{32}B_2Fe_2Ru_2O_7$: C 40.33, H 4.01; found: C 41.27, H 4.21.

Compound 5: ^{11}B NMR (128 MHz, [D$_6$]benzene, 22 °C): $\delta = 121.3$ (s, 1B), 110.6 ppm (s, 1B); ^{1}H NMR (400 MHz, [D$_6$]benzene, 22 °C): $\delta = 8.54$ (br, 2BH$_t$), 1.53 (s, 15H; 1Cp*), 1.51 ppm (s, 15H, 1Cp*); ^{13}C NMR (100 MHz, [D$_6$]benzene, 22 °C): $\delta = 215.1$, 213.9 (CO), 100.9, 99.6 ($C_5(CH_3)_5$), 9.4, 8.2 ppm ($C_5(CH_3)_5$); IR (hexane): $\tilde{\nu} = 2521$ (w, B−Ht), 2005 (w), 1968 (w), 1933 (s), 1726 cm^{-1} (w, CO); MS (FAB): *m*/*z* P^+_{max}: 803; elemental analysis calcd (%) for $C_{27}H_{32}B_2Fe_2Ru_2O_7$: C 40.33, H 4.01; found: C 41.12, H 4.31.

Synthesis of 6: A yellow solution of compound **2** (0.075 g, 0.13 mmol) in hexane (15 mL) was stirred at 70 °C in presence of [$Mn_2(CO)_{10}$] (0.15 g, 0.39 mmol, 3 equiv) for 12 h. All volatiles were removed in vacuo, the residue was extracted into hexane and passed through Celite. The mother liquor was concentrated and the residue was chromatographed on silica-gel TLC plates. Elution with hexane/CH$_2$Cl$_2$ (8:2 v/v) yielded red **6** (0.025 g, 28 %). ^{11}B NMR (128 MHz, [D$_6$] benzene, 22 °C): $\delta = 89.0$ ppm (br, 1B); ^{1}H NMR (400 MHz, [D$_6$]benzene, 22 °C): $\delta = 8.32$ (br, 1BH$_t$), 2.08 (s, 30H; Cp*), −6.37 ppm (s, 1H; Ru-H-Ru); ^{13}C NMR (100 MHz, [D$_6$]benzene, 22 °C): $\delta = 219.3$, 198.0 (CO), 98.3 ($C_5(CH_3)_5$), 8.8 ppm ($C_5(CH_3)_5$); IR (hexane): $\tilde{\nu} = 2498$ (w, B−H$_t$), 2013, 1943, 1736 cm^{-1} (CO). MS (FAB): *m*/*z* P^+_{max}: 707; elemental analysis calcd (%) for $C_{26}H_{32}B_1Mn_1Ru_2O_6$: C 44.08, H 4.55; found: C 42.92, H 4.67.

Synthesis of 7: A yellow solution of [(Cp*Ta)$_2$B$_4$H$_8$(μ-BH$_4$)] (0.04 g, 0.06 mmol) in hexane (10 mL) was stirred in presence of [$Fe_2(CO)_9$] (0.06 g, 0.18 mmol, 3 equiv) at room temperature for 12 h. The solvent was removed in vacuo, the residue was extracted into hexane and passed through Celite. The filtrate was concentrated and kept at −40 °C to remove [$Fe_3(CO)_{12}$]. The mother liquor was concentrated and the residue chromatographed on silica-gel TLC plates. Elution with a hexane/CH$_2$Cl$_2$ (7:3 v/v) mixture yielded **7** (0.005 g, 10 %) and [(Cp*Ta)$_2$B$_5$H$_{11}$] (0.005 g, 12 %). ^{11}B NMR (128 MHz, [D$_6$] benzene, 22 °C): $\delta = 119.5$ ppm (br, 1B); ^{1}H NMR (400 MHz, [D$_6$] benzene, 22 °C): $\delta = 9.4$ (1BH$_t$), 1.82 ppm (s, 30H; Cp*); ^{13}C NMR (100 MHz, [D$_6$]benzene, 22 °C): $\delta = 214.6$, 186 (CO), 100.4 ($C_5(CH_3)_5$), 8.7 ppm ($C_5(CH_3)_5$); IR (hexane): $\tilde{\nu} = 2498$ (w, B−H$_t$), 2017, 1954, 1745 cm^{-1} (CO); MS (FAB): *m*/*z* P^+_{max}: 867; elemental analysis calcd (%) for $C_{26}H_{31}B_1Fe_1Ta_2O_6$: C 35.97, H 3.60; found: C 37.02, H 3.81.

X-ray structural determination: Crystallographic information for the compounds is given in Table 4. The crystal data for **2–4** were collected and integrated using a Bruker AXS Kappa Apex2 CCD diffractometer with graphite-monochromated Mo$_{K\alpha}$ ($\lambda = 0.71073$ Å) radiation at 173 K, and for **6** they were collected and integrated using an Oxford Diffraction Xcalibur-S CCD system equipped with graphite-monochromated Mo$_{K\alpha}$ radiation ($\lambda = 0.71073$ Å) at 150 K. The structures were solved by heavy atom methods using SHELXS-97 or SIR92[61] and refined using SHELXL-97.[62]

CCDC-693478 (**2**), 776024 (**3**), 776025 (**4**), 776026 (**5**) and 776023 (**6**) contain the supplementary crystallographic data for this paper. These data can be obtained free of charge from The Cambridge Crystallographic Data Centre via www.ccdc.cam.ac.uk/data_request/cif.

Acknowledgements

Generous support of the Department of Science and Technology, DST (project no. SR/S1/IC-19/2006), New Delhi is gratefully acknowledged. K.G. and S.K.B. thank the Council of Scientific and Industrial Research (CSIR) and University Grants Commission (UGC), India, respectively, for a Junior and Senior Research Fellowship. We thank Shaikh M. Mobin and V. Ramkumar for X-ray crystallography analysis. We would also like to thank the mass lab, SAIF, CDRI, Lucknow 226001, India for FAB mass analysis.

---

[1] T. P. Fehlner, J.-F. Halet, J.-Y. Saillard, *Molecular Clusters. A Bridge to Solid-State Chemistry*, Cambridge, **2007**.

[2] C. E. Housecroft in *Inorganometallic Chemistry* (Ed.: T. P. Fehlner), Plenum, New York, **1992**.

[3] a) R. N. Grimes, *Acc. Chem. Res.* **1978**, *11*, 420–427; b) R. N. Grimes in *Metal Interactions with Boron clusters* (Ed.: R. N. Grimes), Plenum, New York, **1982**, pp. 269–319; c) R. N. Grimes, *Pure Appl. Chem.* **1982**, *54*, 43–58.

[4] N. N. Greenwood, I. M. Ward, *Chem. Soc. Rev.* **1974**, *3*, 231–271.

[5] a) C. E. Housecroft, *Coord. Chem. Rev.* **1995**, *143*, 297–330; b) C. E. Housecroft, *Boranes and Metalloboranes: Structure, Bonding and reactivity*, Ellis Horwood, Chichester, **1990**, p. 119; c) C. E. Housecroft, *Adv. Organomet. Chem.* **1991**, *33*, 1–50.

[6] a) J. D. Kennedy, *Prog. Inorg. Chem.* **1984**, *32*, 519–670; b) J. D. Kennedy, *Prog. Inorg. Chem.* **1986**, *34*, 211–434; c) J. D. Kennedy in *Disobedient Skeletons* (Ed.: J. Casanova), Wiley, New York, **1998**.

[7] D. F. Gaines in *Recent Advances in the Chemistry of Pentaborane, Vol. 9* (Eds.: R. W. Parry, G. Kodama), Pergamon, Oxford, **1980**.

[8] a) L. Barton, D. K. Srivastava in *Comprehensive Organometallic Chemistry II, Vol. 1* (Eds.: E. Abel, F. G. A. Stone, G. Wilkinson), Pergamon, New York, **1995**, Chapter 8; b) R. N. Grimes in *Comprehensive Organometallic Chemistry II, Vol. 1* (Eds.: E. Abel, F. G. A. Stone, G. Wilkinson), Pergamon, New York, **1995**, Chapter 9.

[9] a) H. Braunschweig, *Angew. Chem.* **1998**, *110*, 1882–1898; *Angew. Chem. Int. Ed.* **1998**, *37*, 1786–1801; b) H. Braunschweig, M. Colling, *J. Organomet. Chem.* **2000**, *614–615*, 18–26; c) H. Braunschweig, M. Colling, *Coord. Chem. Rev.* **2001**, *223*, 1–51; d) H. Braunschweig in *Inorganic Chemical Highlights* (Eds.: G. Mayer, D. Naumann, L. Wesemann), Wiley-VCH, Weinheim, **2001**, pp. 213–218; e) S. Aldridge, D. L. Coombs, *Coord. Chem. Rev.* **2004**, *248*, 535–559; f) D. Vidovic, G. A. Pierce, S. Aldridge, *Chem. Commun.* **2009**, 1157–1171; g) H. Braunschweig, R. D. Dewhurst, A. Schneider, *Chem. Rev.* **2010**, *110*, 3924–3957, and references therein.

[10] H. Braunschweig, T. Wagner, *Angew. Chem.* **1995**, *107*, 904–905; *Angew. Chem. Int. Ed. Engl.* **1995**, *34*, 825–826.

[11] a) H. Braunschweig, C. Kollann, U. Englert, *Angew. Chem.* **1998**, *110*, 3355–3357; *Angew. Chem. Int. Ed.* **1998**, *37*, 3179–3180; b) A. H. Cowley, V. Lomelí, A. Voigt, *J. Am. Chem. Soc.* **1998**, *120*, 6401–6402.

[12] a) H. Braunschweig, M. Colling, *Eur. J. Inorg. Chem.* **2003**, 393–403; b) H. Braunschweig, C. Kollann, D. Rais, *Angew. Chem.* **2006**, *118*, 5380–5400; *Angew. Chem. Int. Ed.* **2006**, *45*, 5254–5274; c) G. Alcaraz, U. Helmstedt, E. Clot, L. Vendier, S. Sabo-Etienne, *J. Am. Chem. Soc.* **2008**, *130*, 12878–12879; d) S. De, G. A. Pierce, D. Vidovic, D. L. Kays, N. D. Coombs, E. D. Jemmis, S. Aldridge, *Organometallics* **2009**, *28*, 2961–2975; e) K. K. Pandey, A. Lledós, F. Maseras, *Organometallics* **2009**, *28*, 6442–6449.

[13] a) C. E. Housecroft, T. P. Fehlner in *Advances in Organometallic Chemistry, Vol. 21* (Eds.: F. G. A. Stone, R. West), Academic Press, New York, **1981**, pp. 57–112; b) T. P. Fehlner in *Electron Deficient Boron and Carbon Clusters* (Eds.: G. A. Olah, K. Wade, R. E. Williams), Wiley, New York, **1991**, p. 287; c) R. N. Grimes, *Chem. Rev.* **1992**, *92*, 251–268.

[14] a) P. L. Timms, *J. Am. Chem. Soc.* **1967**, *89*, 1629–1632; b) P. L. Timms, *Acc. Chem. Res.* **1973**, *6*, 118–123.

[15] H. Braunschweig, *Adv. Organomet. Chem.* **2004**, *51*, 163–192.

[16] a) H. Braunschweig, K. Radacki, D. Scheschkewitz, G. R. Whittell, *Angew. Chem.* **2005**, *117*, 1685–1688; *Angew. Chem. Int. Ed.* **2005**, *44*, 1658–1661; b) D. L. Coombs, S. Aldridge, C. Jones, D. J. Willock, *J. Am. Chem. Soc.* **2003**, *125*, 6356–6357; c) H. Braunschweig, T. Herbst, D. Rais, S. Ghosh, T. Kupfer, K. Radacki, A. G. Crawford, R. M. Ward, T. B. Marder, I. Fernández, G. Frenking, *J. Am. Chem. Soc.* **2009**, *131*, 8989–8999.

[17] H. Braunschweig, K. Radacki, D. Rais, F. Seeler, K. Uttinger, *J. Am. Chem. Soc.* **2005**, *127*, 1386–1387.

[18] H. Braunschweig, D. Rais, K. Uttinger, *Angew. Chem.* **2005**, *117*, 3829–3832; *Angew. Chem. Int. Ed.* **2005**, *44*, 3763–3766.

[19] H. Braunschweig, K. Radacki, D. Rais, F. Seeler, *Angew. Chem.* **2006**, *118*, 1087–1090; *Angew. Chem. Int. Ed.* **2006**, *45*, 1066–1069.

[20] H. Braunschweig, M. Forster, K. Radacki, *Angew. Chem.* **2006**, *118*, 2187–2189; *Angew. Chem. Int. Ed.* **2006**, *45*, 2132–2134.

[21] H. Braunschweig, C. Burschka, M. Burzler, S. Metz, K. Radacki, *Angew. Chem.* **2006**, *118*, 2187–2189; *Angew. Chem. Int. Ed.* **2006**, *45*, 2132–2134.

[22] J. Feilong, T. P. Fehlner, A. L. Rheingold, *Angew. Chem.* **1988**, *100*, 400–402; *Angew. Chem. Int. Ed. Engl.* **1988**, *27*, 424–426.

[23] R. Okamura, K.-I. Tada, K. Matsubara, M. Oshima, H. Suzuki, *Organometallics* **2001**, *20*, 4772–4774.

[24] a) J. F. Hartwig, X. He, *Angew. Chem.* **1996**, *108*, 352–354; *Angew. Chem. Int. Ed. Engl.* **1996**, *35*, 315–317; b) X. He, J. F. Hartwig, *Organometallics* **1996**, *15*, 400–407.

[25] a) C. Dai, G. Stringer, J. F. Corrigan, N. J. Taylor, T. B. Marder, N. C. Norman, *J. Organomet. Chem.* **1996**, *513*, 273–275; b) P. Nguyen, G. Lesley, N. J. Taylor, T. B. Marder, N. L. Pickett, W. Clegg, M. R. J. Elsegood, N. C. Norman, *Inorg. Chem.* **1994**, *33*, 4623–4624; c) T. B. Marder, N. C. Norman, C. R. Rice, E. G. Robins, *Chem. Commun.* **1997**, 53–54.

[26] W. Clegg, F. J. Lawlor, T. B. Marder, P. Nguyen, N. C. Norman, A. G. Orpen, M. J. Quayle, C. R. Rice, E. G. Robins, A. J. Scott, F. E. S. Souza, G. Stringer, G. R. Whittell, *J. Chem. Soc. Dalton Trans.* **1998**, 301–309.

[27] C. N. Iverson, M. R. Smith III, *J. Am. Chem. Soc.* **1995**, *117*, 4403–4404.

[28] a) G. Lesley, P. Nguyen, N. J. Taylor, T. B. Marder, A. J. Scott, W. Clegg, N. C. Norman, *Organometallics* **1996**, *15*, 5137–5154; b) W. Clegg, F. J. Lawlor, G. Lesley, T. B. Marder, N. C. Norman, A. G. Orpen, M. J. Quayle, C. R. Rice, A. J. Scott, F. E. S. Souza, *J. Organomet. Chem.* **1998**, *550*, 183–192.

[29] T. Ishiyama, N. Matsuda, M. Murata, F. Ozawa, A. Suzuki, N. Miyaura, *Organometallics* **1996**, *15*, 713–720.

[30] H. Braunschweig, B. Ganter, *J. Organomet. Chem.* **1997**, *545*, 163–167.

[31] M. Shimoi, S. Ikubo, Y. Kawano, *J. Am. Chem. Soc.* **1998**, *120*, 4222–4223.

[32] a) D. L. Coombs, S. Aldridge, A. Rossin, C. Jones, D. J. Willock, *Organometallics* **2004**, *23*, 2911–2926; b) H. Braunschweig, M. Colling, C. Hu, K. Radacki, *Angew. Chem.* **2003**, *115*, 215–218; *Angew. Chem. Int. Ed.* **2003**, *42*, 205–208; c) H. Braunschweig, M. Forster, K. Radacki, F. Seeler, G. R. Whittell, *Angew. Chem.* **2007**, *119*, 5304–5306; *Angew. Chem. Int. Ed.* **2007**, *46*, 5212–5214; d) H. Braunschweig, M. Forster, T. Kupfer, F. Seeler, *Angew. Chem.* **2008**, *120*, 6070–6072; *Angew. Chem. Int. Ed.* **2008**, *47*, 5981–5983.

[33] a) S. K. Bose, K. Geetharani, B. Varghese, S. M. Mobin, S. Ghosh, *Chem. Eur. J.* **2008**, *14*, 9058–9064; b) S. K. Bose, K. Geetharani, V. Ramkumar, S. M. Mobin, S. Ghosh, *Chem. Eur. J.* **2009**, *15*, 13483–13490.

[34] X. Lei, M. Shang, T. P. Fehlner, *J. Am. Chem. Soc.* **1999**, *121*, 1275–1287.

[35] a) J. Pan, J. W. Kampf, A. J. Ashe III, *Organometallics* **2006**, *25*, 197–202; b) P. Mathur, P. Sekar, *Chem. Commun.* **1996**, 727–728; c) P. Mathur, P. Sekar, A. L. Rheingold, L. M. Liable-Sands, *J. Chem. Soc. Dalton Trans.* **1997**, 2949–2954.

[36] R. Macías, T. P. Fehlner, A. M. Beatty, B. Noll, *Organometallics* **2004**, *23*, 5994–6001.

[37] A. DiPasquale, X. Lie, T. P. Fehlner, *Organometallics* **2001**, *20*, 5044–5049.

[38] Reaction of $[(Cp^*RuH_2)_2B_6H_8]$ and $[(Cp^*M)_2B_5H_9]$ ($M = Mo$ and W) with a series of monometal–carbonyl species were examined, however in no cases was carbonylation observed under the same conditions used for the preparation of **2**. Furthermore, **1** does not react with CO gas to generate **2** under identical conditions.

[39] a) K. Wade, *Adv. Inorg. Chem. Radiochem.* **1976**, *18*, 1–66; b) D. M. P. Mingos, *Nature (London), Phys. Sci.* **1972**, *239*, 16–26; c) D. M. P. Mingos, D. J. Wales, *Introduction to Cluster Chemistry*, Prentice Hall, New York, **1990**.

[40] X. Lei, M. Shang, T. P. Fehlner, *Chem. Eur. J.* **2000**, *6*, 2653–2664.

[41] J. Feilong, T. P. Fehlner, A. L. Rheingold, *J. Organomet. Chem.* **1988**, *348*, C22-C26.

[42] L. N. Pangan, Y. Kawano, M. Shimoi, *Organometallics* **2000**, *19*, 5575–5581.

[43] C. J. Dain, A. J. Downs, G. S. Laurenson, D. W. H. Rankin, *J. Chem. Soc. Dalton Trans.* **1981**, 472–477.

[44] R. Ahmad, J. E. Crook, N. N. Greenwood, J. D. Kennedy, W. S. McDonald, *J. Chem. Soc. Chem. Commun.* **1982**, 1019–1020.

[45] G. A. Pierce, D. Vidovic, D. L. Kays, N. D. Coombs, A. L. Thompson, D. J. Willock, E. D. Jemmis, S. De, S. Aldridge, *Organometallics* **2009**, *28*, 2947–2960.

[46] J. F. Hartwig, S. Huber, *J. Am. Chem. Soc.* **1993**, *115*, 4908–4909.

[47] H. Braunschweig, C. Kollann, U. Englert, *Eur. J. Inorg. Chem.* **1998**, 465–468.

[48] S. Ghosh, M. Shang, T. P. Fehlner, *J. Organomet. Chem.* **2000**, *614-615*, 92–98.

[49] T. A. Albright, J. K. Burdett, M.-H. Whango, *Orbital Interactions in Chemistry*, Wiley, New York, **1985**.

[50] A. A. Aradi, T. P. Fehlner, *Adv. Organomet. Chem.* **1990**, *30*, 189–242.

[51] a) P. Bissinger, H. Braunschweig, F. Seeler, *Organometallics* **2007**, *26*, 4700–4701; b) K. M. Waltz, X. He, C. Muhoro, J. F. Hartwig, *J. Am. Chem. Soc.* **1995**, *117*, 11357–11358.
[52] C. E. Housecroft, T. P. Fehlner, *Adv. Organomet. Chem.* **1982**, *21*, 57–112.
[53] R. Markby, I. Wender, R. A. Friedel, F. A. Cotton, H. W. Sternberg, *J. Am. Chem. Soc.* **1958**, *80*, 6529–6533.
[54] K. Wong, K. J. Haller, T. K. Dutta, D. M. Chipman, T. P. Fehlner, *Inorg. Chem.* **1982**, *21*, 3197–3202.
[55] J. Vites, C. E. Housecroft, C. Eigenbrot, M. L. Buhl, G. J. Long, T. P. Fehlner, *J. Am. Chem. Soc.* **1986**, *108*, 3304–3310.
[56] K. J. Deck, T. P. Fehlner, A. L. Rheingold, *Inorg. Chem.* **1993**, *32*, 2794–2795.
[57] D. P. Tate, W. R. Knipple, J. M. Augl, *Inorg. Chem.* **1962**, *1*, 433–434.
[58] W. J. Schlientz, J. K. Ruff, *Inorg. Chem.* **1972**, *11*, 2265–2267.
[59] C. A. L. Mahaffy, P. L. Pauson, *Inorg. Synth.* **1979**, *19*, 154–155.
[60] G. E. Ryschkewitsch, K. C. Nainan, *Inorg. Synth.* **1974**, *15*, 113–114.
[61] SIR92, Altornare, A. Altomare, G. Cascarano, C. Giacovazzo, A. Guagliardi, *J. Appl. Cryst.* **1993**, *26*, 343–350.
[62] a) SHELXS-97, G. M. Sheldrick, University of Göttingen (Germany), **1997**; b) SHELXL-97, G. M. Sheldrick, University of Göttingen (Germany), **1997**.

Received: May 5, 2010